Accepted 2004 February 3

Terminal velocities of luminous, early-type SMC stars

C. J. Evans[1], D. J. Lennon[1], C. Trundle[1,2], S. R. Heap[3], D. J. Lindler[3]

ABSTRACT

Ultraviolet spectra from the Space Telescope Imaging Spectrograph (STIS) are used to determine terminal velocities for 11 O and B-type giants and supergiants in the Small Magellanic Cloud (SMC) from the Si IV and C IV resonance lines. Using archival data from observations with the Goddard High-Resolution Spectrograph and the *International Ultraviolet Explorer* telescope, terminal velocities are obtained for a further five B-type supergiants. We discuss the metallicity dependence of stellar terminal velocities for supergiants, finding no evidence for a significant scaling between Galactic and SMC metallicities for $T_{\rm eff} < 30{,}000\,$K, consistent with the predictions of radiation driven wind theory. A comparison of the v_∞/v_{esc} ratio between the SMC and Galactic samples, while consistent with the above statement, emphasizes that the uncertainties in the distances to galactic OB-type stars are a serious obstacle to a detailed comparison with theory. For the SMC sample there is considerable scatter in v_∞/v_{esc} at a given effective temperature, perhaps indicative of uncertainties in stellar masses.

Subject headings: Galaxies: individual: Magellanic Clouds – stars: fundamental parameters – stars: winds, outflows – stars: early-type

1. Introduction

Observations of individual early-type stars in the Small Magellanic Cloud (SMC) facilitate studies of stellar evolution and radiatively driven winds in a metal-poor environment.

[1]Isaac Newton Group of Telescopes, Apartado de Correos 321, 38700 Santa Cruz de la Palma, Canary Islands, Spain.

[2]Dept. of Pure and Applied Physics, Queen's University of Belfast, Belfast, BT7 1NN, N. Ireland, UK.

[3]Laboratory for Astronomy and Solar Physics, Code 681, NASA Goddard Space Flight Center, Greenbelt, MD 20771.

Stellar winds are thought to be driven by momentum transfer from metal line absorption; thus, one would *expect* global wind properties to be dependent on metallicity (Z). Partial confirmation of this is offered from morphological consideration of SMC ultraviolet spectra in which P-Cygni type profiles are weaker (or even absent) when compared with Galactic analogs (e.g., Walborn et al., 2000). Previous UV surveys using the *International Ultraviolet Explorer* telescope (*IUE*; Garmany & Conti, 1985) and the *Hubble Space Telescope* (*HST*; Walborn et al. 1995) concluded that terminal velocities (v_∞) for early-type stars are on average lower in the SMC than in their Galactic counterparts. This finding has subsequently been echoed by Kudritzki & Puls (2000) and Puls, Springmann, & Lennon (2000), albeit based on the same observational data. In addition, a theoretical prediction by Leitherer, Robert, & Drissen (1992) that v_∞ scales as $Z^{0.13}$ is at times referred to in the literature as having been confirmed (e.g., Vink, de Koter, & Lamers 2001).

A detailed analysis of the line driving process for radiatively driven winds, including its dependence on metallicity, was given by Puls et al. (2000). They note that, to first order,

$$v_\infty/v_{esc} \sim \frac{\hat{\alpha}}{1-\hat{\alpha}}, \tag{1}$$

where $\hat{\alpha}$ is the effective value of the force multiplier parameter, α, defined as the exponent of the line strength distribution function. This parameter depends on both metallicity and depth (temperature and density) and Puls et al. give explicit examples at various effective temperatures and metallicities. Provided that we do not enter the regime of weak winds, their Figure 27 illustrates that for O-stars ($\mathrm{T_{eff}} = 40,000\,\mathrm{K}$) the value of $\hat{\alpha}$ is only weakly dependent on metallicity, at least down to one tenth solar. This is confirmed by the calculations of Kudritzki (2002), who parameterized the temperature and density variations of the force multiplier parameters to construct wind models for O-type stars to very low metallicity ($0.0001\ Z_\odot$). From Kudritzki's Table 2 and Figure 9 we see that, at the metallicity of the SMC, one does not expect any significant change in the value of v_∞/v_{esc} for very luminous O-type stars (in fact, for the lowest surface gravity models there is even a small increase in terminal velocity as metallicity is changed from solar to one-fifth solar). This result does not necessarily contradict Leitherer et al., who note that their scaling is a description of the average behavior and that "v_∞ may increase with decreasing Z in certain $T_{\rm eff}$ domains" as a result of varying ionization conditions in the wind. For the Kudritzki main-sequence models there is indeed a weak trend with Z, which essentially agrees with the Leitherer et al. scaling (which for one-fifth solar implies a change of only 20%, comparable to the uncertainty arising from the determination of the surface gravities).

In part prompted by the Kudritzki results, here we attempt a more quantitative investigation of terminal velocities for supergiants in the SMC; we determine v_∞ for a total of 16 targets. Aside from consideration as a whole to study the effects of metallicity, such results

are useful individually. Terminal velocities are a necessary "ingredient" for the detailed atmospheric analyses now possible for early-type stars. Theoretical model atmosphere codes have undergone significant development over the past decade, most recently with the inclusion of line-blanketing arising from metallic species e.g., CMFGEN (Hillier & Miller, 1998) and FASTWIND (Santolaya-Rey, Puls, & Herrero 1997; Herrero, Puls, & Najarro 2002). One of the most salient results from the application of these codes to analyses of O-type stars is the downward revision of stellar temperatures (when compared with previous determinations that did not include the effects of blanketing), noted for plane-parallel models by Hubeny, Heap, & Lanz (1998). This effect has since been more thoroughly explored in both the Galaxy and the Magellanic Clouds using extended atmospheres e.g., Martins, Schaerer, & Hillier (2002), Crowther et al. (2002), Herrero et al. (2002) and Bouret et al. (2003).

Detailed line-blanketed methods have currently not been applied widely to B-type stars. In combination with high-resolution optical data from the VLT UV-Visual Echelle Spectrograph (UVES), the v_∞ results presented here for four of our early B-type Space Telescope Imaging Spectrograph (STIS) targets are used by Trundle et al. (2004, hereafter TL04) to determine intrinsic stellar and wind parameters using FASTWIND. Part of our motivation in addressing the dependence of terminal velocities on environment also stems from the TL04 study. Ultraviolet spectra of four further SMC targets (observed as part of the same STIS program) do not display evidence of strong stellar winds and the methods we use here are not sufficient for determination of v_∞ (these additional data will be discussed in a subsequent paper). We therefore investigate the scaling relation of v_∞ with stellar escape velocity ($v_{\rm esc}$), with a view to obtaining estimates of the terminal velocities for these additional targets. We note that such scaling relations are also of interest as they are employed in the analysis of samples of stars which are too distant or numerous to obtain UV spectra (e.g, Urbaneja et al. 2003).

2. Observations

2.1. *HST*-STIS observations

In the course of our *HST* General Observer programs (GO7437 and GO9116, P.I.: DJL) we have observed a number of O and B-type SMC stars that display evidence of strong stellar winds, for which terminal velocities can be determined. The dwarfs in the young cluster NGC 346 (observed as part of G07437) have recently been studied by Bouret et al. (2003) and are not considered here. Observational details of our 11 targets are summarized in Table 1; all are drawn from the catalog of Azzopardi & Vigneau (AzV; 1975, 1982).

Each target was observed using the STIS in echelle mode, with the far-UV MAMA (Multi-Anode Microchannel Array) detector and the E140M grating (centered at 1425 Å); those from program GO9116 were also observed with the near-UV MAMA and the E230M grating (centered at 1978 Å). All of the observations were made through the $0\farcs2 \times 0\farcs2$ entrance aperture and the effective spectral resolving power of the E140M and E230M gratings are $R = 46,000$ and 30,000, respectively. The exposure times for the GO9116 data were set from consideration of low-resolution *IUE* spectra. With the E140M grating the exposure times range from 54 to 216 minutes (Sk 191 and AzV 18, respectively), with shorter exposures for the E230M set-up (ranging from 38 to 75 minutes).

The primary CALSTIS processing steps are described by Walborn et al. (2000), with the difference here that the two-dimensional inter-order background correction performed manually in those reductions has now been incorporated into the standard pipeline as SC2DCORR. After pipeline reduction the individual echelle orders were extracted and merged to form a continuous spectrum. Prior to merger (typically) 25 pixels at both ends of each order are clipped; the spectral overlap between orders is generally large enough to accommodate this and the final result has a more consistent signal-to-noise ratio than otherwise. The reduced echelle spectra cover the wavelength ranges 1150-1700 Å (E140M) and 1600-2350 Å (E230M). For display purposes (and for consistency with Walborn et al. 2000) the spectra are binned to 0.25 Å per data point. The S/N (on the basis of photon statistics) is typically in the range of 20-30 per binned data point.

In Table 1 we also give H I column densities, N(H I), toward our targets, found assuming the Lyα profile arises from a pure damping profile (see e.g., Shull & Van Steenberg 1985 and references therein). To avoid possible contamination by the N V $\lambda\lambda$1239, 1243 doublet, we consider only the blueward wing when deriving the tabulated values.

2.1.1. Multiplicity of AzV 47 and 216

Target acquisition images used for the STIS are taken using a 100×100 pixel CCD camera (covering $5''\times5''$), with the "longpass" broad-band filter centered at 7230 Å (FWHM = 2720 Å). Inspection of these images for each of our targets generally show isolated point sources, with the exception of a faint companion present in the image of AzV 47. While inspecting the acquisition data from the additional targets observed for program GO9116,[1] it came to our attention that the acquisition image for AzV 216 (classified as B1 III by TL04) also displays

[1]Lower luminosity targets were also observed for compilation of spectral libraries and their UV spectra are not discussed here.

a faint companion. These images are shown in Figure 1.

The separations are ∼3 pixels (0.15″) in AzV 47 and ∼5 pixels (0.25″) in AzV 216 which, at the distance of the SMC, corresponds to approximately 9000 and 15,000 AU, respectively; both companions are relatively faint in comparison to the primary targets. Some contamination is possible in the UV spectrum of AzV 47 because the companion will not be excluded by the 0.″2 × 0.″2 aperture. However, Walborn et al. (2000) noted that "the optical and UV spectra of AzV 47 are entirely normal for its type," so it is likely that there is not a significant contribution from the companion. A full analysis of the VLT-UVES spectrum of AzV 216 is presented by TL04; both Hα and the He I λ4471 line show some asymmetry, likely originating from the presence of a nearby companion.

2.2. Additional UV data

To augment the *HST*-STIS spectra, we include four B1-type stars observed with the *HST* using the Goddard High-Resolution Spectrograph (GHRS) as part of program GO6078 (P.I.: DJL). We also include a high-resolution observation of AzV 78 made with the *IUE* telescope using the large aperture with the short-wavelength prime (SWP) camera (image SWP09334, Fitzpatrick & Savage, 1985). The GHRS observations do not cover the Lyα region, and, although the spectrum of AzV 78 extends far enough into the blue, the signal-to-noise in the region of Lyα is not sufficiently high to permit measurement of the H I column density. These additional targets are also detailed in Table 1.

3. Determination of terminal velocities: SMC stars

The stellar winds of B-type stars are much less intense than those observed in O-type stars; terminal velocities (e.g, Prinja, Barlow, & Howarth 1990) and mass-loss rates (e.g., Kudritzki et al. 1999) are generally both lower in B-type stars. P Cygni–like profiles are seen in the Si IV and C IV resonance lines of three stars (AzV 210, 215, and Sk 191), and weak Si IV emission is seen in AzV 18. Terminal wind velocities were determined for these four stars using the Sobolev with Exact Integration (SEI) computer program developed by Haser (1995). This program was then employed to find v_∞-values for the seven O-type STIS targets in Table 1 and for the five archival GHRS/*IUE* B-type spectra. The same SEI program has been widely used in other recent analyses of early-type stars in the Local Group, e.g., Herrero et al. (2001, Milky Way), Bresolin et al. (2002, M31), and Urbaneja et al. (2002, M33).

The SEI code adopts a standard β-law to describe the velocity structure and includes a turbulent velocity, which increases with radius to a maximum of $v_{\rm turb}$ at v_∞ (see Haser et al., 1995 for further details). The C IV $\lambda\lambda$1548.19, 1550.76 and Si IV $\lambda\lambda$1393.73, 1402.73 doublets are used as diagnostics of v_∞. We do not use the N V $\lambda\lambda$1238.81, 1242.80 doublet in our analysis as a consequence of its weakness in early B-type spectra (which constitute the bulk of our sample) and because of problems arising from its contamination by Lyα absorption. The adopted β-law is essentially a free parameter in the SEI program, to be determined from morphological comparisons of the observed and theoretical resonance lines. In the current work we are solely interested in the terminal velocity and, though small variations in β can lead to more aesthetically pleasing line fits, the resulting v_∞-values are still within the quoted errors. Therefore, in contrast to other studies (e.g., Bresolin et al., 2002), we do not attempt to "fit" the β-law for our targets and adopt $\beta = 1$ (consistent with the results of e.g., Massa et al. 2003).

Our results are given in Table 1, and model fits for four of our B-type STIS targets are shown in Figure 2. To correct for the underlying photospheric components of the resonance lines in our analysis, we use archival *IUE* observations of B-type stars with low projected rotational velocities (selected from Siebert, 1999) as templates,[2] convolved by the appropriate $v \sin i$ of each target (for estimates see TL04 and Walborn et al. 2000). The model spectra were also convolved with an instrumental broadening function, although given the high resolution of these data this effectively has no impact on the derived velocities.

Terminal velocities for the B-type spectra are determined primarily from consideration of the Si IV doublet. However, as shown in the top panel of Figure 2, we are unable to match the morphology of the Si IV doublet in AzV 215. The presence of the relatively flat "shelf" resembles that seen in κ Ori (HD 38771, B0.5 Ia, Walborn, Nicols-Bohlin, & Panek 1985) though in AzV 215 it is more extreme. The C IV profile for this star is shown in Figure 3 and is well matched by a $v_\infty = 1400$ km s^{-1} model.

In determining v_∞ for our O-type spectra we use the C IV profile as the primary diagnostic; the Si IV doublet is a relatively weak feature in the O-type stars studied here (see Walborn et al. 2000). Correcting for the photospheric component is complicated in O-type stars by the absence of templates uncontaminated by stellar winds (the same problem is discussed by Massa et al. 2003). In Figure 3 we show model fits for two of our O-type spectra (AzV 75 and 95) and also for AzV 215. In the case of AzV 215 the same v_∞-value is found regardless of whether the photospheric correction is included (using υ Ori, HD 36512, Wal-

[2]Additional tests with new SMC metallicity TLUSTY models (R. Ryans, 2003, private communication) yield essentially identical terminal velocities.

born et al. 1985), i.e., the large terminal velocity of the wind leaves the blue-edge relatively free of photospheric contamination. To test if this also holds true for our O-type stars we used the *IUE* spectrum of the subluminous dwarf BD+75 325 (classified as O5p [Gould, Herbig, & Morgan 1957] and used by Herrero et al., 2001, in analysis of their hottest stars) as a template for AzV 75 and 95. As demonstrated in Figure 3, the blue edge of the C IV profile is again largely independent of the inclusion of a photospheric template, although a more visually pleasing fit is achieved to the emission profile. For the remaining O-type stars we simply match the blue edge, without including a photospheric template.

It is important to note that the determination of the best fit in all our spectra is subjective. In the case of saturated lines different combinations of v_∞ and $v_{\rm turb}$ can be used to match the blue wing of the profiles; in nonsaturated, weaker lines the adopted line-strength of each doublet is an additional parameter to be considered. Typical uncertainties in v_∞ are $\pm\,100\,$km s^{-1}, except in the case of the four B-type stars with $v_\infty < 500$km s^{-1}, where it is in the region of $\pm\,50\,$km s^{-1}.

3.1. Comparison with previous results

Terminal velocities for three of our targets were determined by Prinja (1987) from comparison of low-dispersion *IUE* spectra with theoretical profiles. His value for AzV 242 (1000 km s^{-1}) is within our quoted uncertainty, though his result for AzV 215 (1675 km s^{-1}) is slightly larger. More worrying is that his value for Sk 191 (850 km s^{-1}) is twice our result. This prompted us to retrieve the relevant *IUE* spectrum from the archive and it neither displays P-Cygni emission nor saturated absorption profiles. From the new higher quality STIS data, measurement of the blueward limit of the saturated core of both the C IV and Si IV doublets (generally referred to as v_{black} in the literature) gives a velocity of 450 km s^{-1}, proscribing the larger result.

A more recent study of AzV 242 (Prinja & Crowther, 1998) gives $v_\infty = 860$km s^{-1} from consideration of observed narrow absorption components (NACs; a method we do not pursue here). Albeit at the lower limit, this result is again within our expected uncertainty.

Garmany & Fitzpatrick (1988) also used low-dispersion *IUE* spectra to study a sample of SMC stars and there is some overlap with our targets (namely AzV 15, 69, 75, and 95). They were limited to estimates of the terminal velocities, in effect measuring a v_{edge} (usually defined as where the absorption component of the P-Cygni profile meets the continuum). We do not consider such measurements here; the relation of v_{edge} to v_∞ is dependent on the morphology of the blueward part of the profile, which is primarily determined by the tur-

bulent velocity. As one would expect, their velocities are considerably larger ($\sim$500 km s^{-1}) than those from the new analyses.

Finally, detailed non-LTE, line-blanketed model atmosphere analyses of AzV 69 and 83 were presented by Hillier et al. (2003). From fitting the absorption and emission line widths of selected UV lines, terminal velocities of 1800 km s^{-1}(AzV 69) and 940 km s^{-1}(AzV 83) were obtained from comparisons with model spectra; these results are well within the quoted uncertainties when compared with our new SEI results in Table 1.

4. Determination of terminal velocities: Galactic stars

To provide a test of our methods we have also used the SEI program to determine terminal velocities for five Galactic B-type supergiants taken from the Walborn et al. (1985) *IUE* atlas. These stars are drawn from the sample of $\sim$60 early B-type supergiants analysed by Haser (1995), and a comparison of results is given in Table 2. The velocities determined here are *smaller* than those found by Haser, and consequently the adopted turbulent velocities are larger (to match the blue edge of each line as described in §3).

In their analyses of O-type stars Groenewegen & Lamers (1989), Haser (1995), and Massa et al. (2003) adopted turbulent velocities in the range 0.05-0.15 v_∞. Comparable results are found for the O-type stars studied here, with the exception of AzV 83. Haser used similar turbulent velocities for his B-type sample (i.e., 0.05-0.15 v_∞). This highlights a potential difference in methods between Haser's and the current study; our adopted turbulent velocities are generally larger. Both Bresolin et al. (2002) and Urbaneja et al. (2002) also noted that $v_{\rm turb}/v_\infty$ was larger for their analyses of B-type spectra, compared with previous O star results.

One factor contributing to the larger ratio is simply that the terminal velocities in the cooler B-type stars are typically smaller than those in the O stars. Coupled with the fact that $v_{\rm turb}$ does not appear to vary systematically with spectral type this leads to a larger $v_{\rm turb}/v_\infty$ ratio. However, inspection of Table 2 highlights an important issue that arises from our Galactic analyses. In all five cases we adopt larger turbulent velocities than Haser to match the same observations, using the same program. The situation is most severe in HD 152236, where $v_{\rm turb}$ is a factor of 4 larger. In Figure 4 we compare our fit to the HD 152236 Si IV doublet with a model calculated using the parameters found by Haser. The larger turbulent velocity adopted in our study is clearly more consistent with the blue-edge of each component than in the Haser model; note also that the width of the absorption profile is better matched by our model. The same features are present when comparing the other four *IUE* targets

with models calculated with Haser's values. The Haser v_∞ results are generally at the "upper limit" of our results, suggesting that his methods were slightly different; i.e., he found the maximum velocity consistent with the data, whereas our approach has been to find the range of v_∞ (for which reasonable fits are found) and then taking the central value. These results highlight the dependence of the derived terminal velocity on the adopted turbulence. We emphasize that $v_{\rm turb}$ in the present context is used very much as a fitting parameter, the physical interpretation of such large turbulent velocities is extremely uncertain.

As an aside, we note that the *IUE* image used for our analysis of HD 91969 is not that from the Walborn et al. atlas (SWP06510). Haser did not specify which image was used in his analysis, but his v_∞ of 1550 km s^{-1} is comparable with previous results from SWP09076, i.e., 1545 km s^{-1} (Prinja et al., 1990) and 1500 km s^{-1} (Lamers, Snow, & Lindholm 1995). The wind variability of HD 91969 has been discussed recently by Prinja, Massa, & Fullerton (2002) and is highlighted by our results; for the SWP09076 spectrum we find $v_\infty = 1500$ km s^{-1}, cf. 1350 km s^{-1} from SWP06510.

5. Discussion

The correlation between terminal and stellar escape velocities was noted by Abbott (1978) and subsequent studies (e.g., Groenewegen, Lamers, & Pauldrach, 1989; Howarth & Prinja, 1989; Lamers et al. 1995) have revisited this relationship. A reliable, well-constrained v_∞/v_{esc} relation is an extremely attractive prospect. For instance, if the wind momentum-luminosity relationship (WLR, e.g., Kudritzki & Puls 2000) is to be used to determine distances to galaxies beyond the Local Group, ultraviolet stellar spectra are generally not available (e.g, Urbaneja et al. 2003). In comparison with theoretical spectra, optical data can be used to provide an initial estimate of v_{esc}, thence an estimate of v_∞, with some iteration to a final solution. Before investigating this relationship for our SMC sample, we compare our v_∞ results with those from Galactic studies.

5.1. Terminal velocities

Common belief holds that terminal velocities in the SMC will be lower than in the Galaxy because of the decrease in metallicity (e.g., Kudritzki & Puls, 2000). Kudritzki & Puls presented a comparison of terminal velocities (as a function of temperature) for Galactic and Magellanic Cloud targets. A necessary step in this process was the adoption of a suitable calibration to allocate effective temperatures to a given spectral type (in their

case that of Humphreys & McElroy, 1984). Over the past 20 years, significant developments have been made in model atmosphere techniques, most recently the downward revision of the temperature scale discussed earlier owing to the inclusion of line blanketing (e.g., Martins et al. 2002). If we are to compare our v_∞-values with Galactic results in this manner, it is clear that any differences in temperature scales should be minimized.

Temperatures for the SMC targets are taken from line-blanketed, non-LTE analyses by Hillier et al. (2003; AzV 69, 83), TL04 (Sk 191, AzV 18, 210, 215), and Trundle et al. (2004, in preparation; AzV 78, 242, 264); note that for consistency with the analysis of AzV 69 and 83 by Hillier et al. we adopt their v_∞-values. Temperatures for the remaining targets (AzV 15, 75, 95, 327)[3] are estimated from interpolation between the line-blanketed results of Crowther et al. (2002) and Martins et al. (2002). Our results are supplemented by those from similar analyses of SMC targets by Crowther et al. (2002; AzV 232) and Evans et al. (2004; AzV 70, 235, 372, 456, 469, 488). Terminal velocities for this expanded sample are plotted as a function of stellar effective temperature ($T_{\rm eff}$) in Figures 5 and 6.

In Figure 5 we compare our results with the data of Lamers et al. (1995). Their O-type temperatures were taken from the unpublished Garmany catalog and Chlebowski & Garmany (1991), in which non-LTE results were used to define a temperature scale. Temperatures for their B-type targets were taken from the LTE calibrations of Schmidt-Kaler (1982). From qualitative inspection of Figure 5 it appears as though the SMC values are generally lower than the Galactic values, as previously assumed in the literature.

In Figure 6 we show our results together with recent results from detailed analysis of individual Galactic targets, i.e., independent of any external temperature calibrations. Results for O-type supergiants (and giants) are taken from the non-LTE, line-blanketed studies of Herrero et al. (2002) and Repolust, Puls, & Herrero (2004). TL04 presents such analyses for B-type SMC supergiants, but there are no contemporary results for Galactic B stars. In Figure 6 we include results from McErlean et al. (1999), which employed non-LTE methods to analyze Galactic B-type stars, but which predate the availability of line-blanketed atmosphere codes; v_∞ values are taken from Haser (1995) or Howarth et al. (1997). As discussed in TL04, for the early B-type spectra the inclusion of line-blanketing has a relatively minor effect on the temperature scale (cf. the results of Dufton et al. 2000), i.e., McErlean's temperatures are preferable to those assumed from Schmidt-Kaler.

In contrast to the comparison with the Lamers et al. sample, there is no obvious *qualitative* difference between the Galactic and SMC results for $T_{\rm eff} < 30,000\,{\rm K}$. Linear

[3]We omit AzV 80 from this discussion since the exact nature of the peculiar "nfp" spectral class is unclear (Walborn et al. 2000).

fits to these results (excluding the Galactic A-type supergiants) give slightly different relations for the Galactic and SMC samples. However, because of the scatter of the results, these differences are not statistically significant and therefore we do not undertake a rigorous quantitative analysis.

At hotter temperatures the situation is somewhat more ambiguous; our motivations for the current study were primarily concerned with B-type supergiants and the sampling of targets with $T_{\rm eff} > 30,000\,{\rm K}$ is relatively sparse. In Figure 6 we distinguish between luminosity class I and III objects. With the exception of the low velocity for HD 191423, the Galactic giants *appear* to have generally larger v_∞-values than the Galactic supergiants. A more objective comment is that v_∞ for the SMC giants is lower than for the Galactic targets (again excepting HD 191423), although from such a limited sample such differences clearly cannot be attributed to the change in metallicity. We are similarly limited by our sample of more luminous O-type stars. Both AzV 83 and 232 have low terminal velocities for their spectral types (noted by Walborn et al. 2000) and appear distinctly different from the Galactic supergiants. However AzV 83 and 232 are both "Iaf" type spectra with dense winds (e.g., Hillier et al. 2003); v_∞-values for similarly extreme stars in the LMC are also relatively low, e.g., Sk $-66°169$ (Crowther et al. 2002, Massa et al. 2003). The Galactic supergiants in Figure 6 are less extreme objects and therefore do not permit a sensible direct comparison of O-type supergiant terminal velocities at the current time.

5.2. Stellar escape velocities

We now consider the escape velocities for SMC stars with published intrinsic stellar parameters (see Table 3). As is usual in such studies, we define the *effective* escape velocity (v_{esc}) as the gravitational escape velocity, corrected for the contribution to the radiative acceleration caused by Thomson scattering by free electrons. Therefore,

$$v_{esc} = \sqrt{\frac{2GM_*(1-\Gamma)}{R_*}} \tag{2}$$

where Γ is the ratio of the radiative acceleration from electron scattering to the stellar gravity given by

$$\Gamma = \frac{\sigma_e L_*}{4\pi G M_* c} \tag{3}$$

in which σ_e is the electron scattering opacity, given by $n_e\sigma_{\rm T}/\rho$, where n_e is the electron number density, $\sigma_{\rm T}$ is the Thomson cross-section, and ρ is the density of the gas. From the TL04 FASTWIND model for AzV 215, $\sigma_e = 0.31$ (at $\tau = 2/3$). This value is consistent

with previous values in early-type stars (e.g., using equation (3) and their values for Γ, σ_e = 0.28–0.32 in the Galactic study of Lamers et al., 1995) and is used here in our calculations.

Stellar radii, masses, and luminosities are taken from the relevant papers; note, however, that the SMC distance modulus adopted by Hillier et al. was 19.1 (cf. 18.9 in the other studies) which will affect the luminosity of the final atmospheric models, hence the radii and masses and ultimately the escape velocity (of order 10%).

In Figure 7 we compare $v_\infty/v_{\rm esc}$ for the SMC stars in Table 3 with the results from Lamers et al. (1995). As discussed before in §5.1, the temperature scales are not directly comparable but both the scatter and the mean value of $v_\infty/v_{\rm esc}$ is roughly consistent with that of the Lamers sample. From a compilation of published results, Kudritzki & Puls (2000) found $v_\infty = 2.65\,v_{esc}$ ($T_{\rm eff} \geq$ 21,000 K) quoting an accuracy of $\sim 20\,\%$. The mean from our sample (excluding AzV 18 and 210 as they are cooler than 21,000 K) is 2.36; AzV 83 is again the most distant outlier.

In Figure 8 our results are compared with those for Galactic O-type giants/supergiants (Herrero et al. 2002; Repolust et al. 2004) and B and A-type supergiants (Kudritzki et al. 1999). The results for HD 207198 and 209975 (Repolust et al. 2004; $v_\infty/v_{\rm esc}$ = 6.09 and 5.62, respectively) are excluded from the figure. These two stars are listed by Markova et al. (2004) as being members of the Cep OB2 association, for which they adopt a distance of 0.85 kpc. However, *Hipparcos* results by de Zeeuw et al. (1999) support a smaller distance of 0.62 kpc. The region is also extended over several degrees, so there will likely be a significant depth effect within the association, leading to uncertain relative distances. From equation (2) overestimates of their luminosities will lead to underestimates of v_{esc}. Smaller distances for these two stars would bring them into better agreement with the other results in Figure 8. The mean v_∞/v_{esc} of the remaining Galactic targets ($T_{\rm eff} \geq$ 21,000 K) is 3.07, more in keeping with Abbot's (1978) suggestion that $v_\infty \sim 3v_{esc}$ than the Kudritzki & Puls result.

Uncertainties in the distances to the Galactic targets may contribute to these differing results and also to the greater spread of $v_\infty/v_{\rm esc}$ (cf. Lamers et al.). However, it is worth noting that the targets in the Herrero et al. (2002) study are all (thought to be) members of Cyg OB2; aside from any systematic offset, the spread of results for their seven targets should be minimized and yet a wide range of $v_\infty/v_{\rm esc}$ is still found. Unfortunately, from current methods there will always be a large scatter associated with v_∞/v_{esc}, primarily a result of the uncertainty in $\log g$ of (at least) ± 0.1 dex. This corresponds to a large uncertainty in the spectroscopic mass, which in the case of, e.g., AzV 215, yields results for v_{esc} of $\pm\,20\,\%$.

In addition to its use for targets without ultraviolet information, understanding the scaling of v_∞ with v_{esc} is useful for targets such as AzV 22 and 362 (see TL04 for analysis).

The optical spectra of these two stars display evidence of a stellar wind, but their ultraviolet spectra (also observed as part of GO9116) are devoid of strong wind signatures. Similarly, infilling of the Hα profiles is observed in AzV 104 and 216 indicative of some, albeit weak, stellar wind. Since we are limited in the current work by a relatively small sample, TL04 used the Kudritzki & Puls formula to obtain v_∞ estimates for inclusion in FASTWIND.

In general, the results in Figure 8 display no evidence for a significantly different $v_\infty/v_{\rm esc}$ ratio in the SMC in comparison with that for Galactic stars. We therefore conclude that in the case of supergiants with strong winds, our results are in good agreement with predictions of theory.

Figures 7 and 8 also prompt further discussion in the context of the so-called "bistability jump" near $T_{\rm eff} = 21{,}000$ K (Lamers et al. 1995). From Figure 7, there appears to be a clear step between the high (hotter) and low (cooler) ionization regimes, but such a well-defined edge is largely an artifact of the temperature assignment for the spectral bins. The Lamers et al. sample includes seven B1-type stars for which the same temperature (20,800 K) is used; in reality, the temperature for a given spectral type encompasses a range of values, e.g., Sk 191 and AzV 210 are both B1.5 Ia-type spectra, yet their temperatures differ by 2000 K (TL04). Further complications can arise from the effects of line-blanketing, i.e., the temperature derived for a star with a strong wind can be lower than that found for a later spectral type with a much weaker wind. In these cases the temperature scale is not necessarily monotonic (e.g., TL04, Evans et al. 2004) and the temperature range for a given spectral type can overlap with that of another. In Figure 8 there is still evidence for a lower $v_\infty/v_{\rm esc}$ ratio at cooler temperatures, but, as a consequence of analysing individual stars rather than employing an effective temperature-spectral type calibration, the boundary is somewhat "blurred." Additionally, we note that the median $v_\infty/v_{\rm esc}$ for those SMC stars significantly hotter than this region ($T_{\rm eff} > 24{,}000$ K) is 2.63, consistent with the Kudritzki & Puls relation.

6. Conclusions

From high-quality ultraviolet spectra we have used the SEI method to determine terminal velocities for nine B-type supergiants and seven O-type stars in the SMC. One important conclusion from the current work is that, if one is solely interested in terminal velocities, many of the parameters in the SEI code are essentially cosmetic fitting parameters to which other authors have attributed undue significance in previous studies.

We compare our results with those from recent Galactic studies, adopting temperatures

from tailored atmospheric analyses, independent of external calibrations. To our knowledge, this is the first time such a thorough comparison has been made, giving a clearer view of the scaling of terminal velocities. We find no evidence for lower terminal velocities in the SMC than in the Galaxy for $T_{\rm eff} < 30{,}000$ K (corresponding to spectral types later than O9). Similarly, in agreement with the predictions of theory for luminous supergiants, we find no evidence for a significantly different scaling of v_∞ with $v_{\rm esc}$ in the SMC in comparison with that in the Galaxy. We stress that the situation for giants and dwarfs remains untested.

From our limited sample it appears that v_∞ for O-type giants may be lower in the SMC than in the Galaxy, although both this and the situation for O-type supergiants warrants further investigation. Further results from contemporary model atmosphere analyses of O-type stars in the Galaxy and the Magellanic Clouds would greatly help attempts to delineate the scaling of v_∞ with both temperature and v_{esc}.

Finally, given the uncertain distances, it would appear that calibrating the WLR using Galactic OB-type stars is not an attractive prospect at the current time.

7. Acknowledgements

CJE (under grant PPA/G/S/2001/00131) and DJL acknowledge financial support from the UK Particle Physics and Astronomy Research Council (PPARC). CT is grateful to the Department of Higher and Further Education, Training, and Employment for Northern Ireland (DEFHTE) and the Dunville Scholarships fund for their financial support. Based in part on observations with the NASA/ESA *Hubble Space Telescope* obtained at the Space Telescope Science Institute, which is operated by the Association of Universities for Research in Astronomy, Inc. and on INES data from the *IUE* satellite. We thank Miguel Urbaneja for his useful initial assistance with the SEI program and Robert Ryans for the TLUSTY models. We also thank both Alex Fullerton and the referee for their helpful comments on the manuscript.

REFERENCES

Abbott D. C., 1978, ApJ, 225, 893

Azzopardi M. & Vigneau J., 1975, A&AS, 22, 285

Azzopardi M. & Vigneau J., 1982, A&AS, 50, 291

Bouret J.-C., Lanz T., Hillier D. J. et al., 2003, ApJ, 595, 1182

Bresolin F., Kudritzki R.-P., Lennon D. J. et al., 2002, ApJ, 580, 213

Chlebowski, T., Garmany C. D., 1991, ApJ, 368, 241

Crowther P. A., Hillier D. J., Evans C. J. et al., 2002, ApJ, 579, 774

de Zeeuw P. T., Hoogerwerf R., de Bruijne J. H. J. et al., 1999, AJ, 117, 354

Dufton P. L., McErlean N. D., Lennon D. J., Ryans R. S. I., 2000, A&A, 353, 311

Evans C. J., Crowther P. A., Fullerton A. W., Hillier D. J., 2004, ApJ, submitted

Fitzpatrick E. L., Savage B. D., 1985, ApJ, 292, 122

Garmany C. D., Conti P. S., 1985, ApJ, 293, 407

Garmany C. D., Conti P. S., Massey P., 1987, AJ, 93, 1070

Garmany C. D., Fitzpatrick E. L., 1988, ApJ, 332, 711

Gould N. L., Herbig G. H., Morgan W. W., 1957, PASP, 69, 242

Groenewegen M. A. T., Lamers H. J. G. L. M., 1989, A&AS, 79, 359

Groenewegen M. A. T., Lamers H. J. G. L. M., Pauldrach A. W. A., 1989b, A&A, 221, 78

Haser S. M., 1995, Ph.D. thesis, Univ. of Munich

Haser S. M., Lennon D. J., Kudritzki R.-P. et al., 1995, A&A, 295, 136

Herrero A., Puls J., Corral L. J. et al., 2001, A&A, 366, 623

Herrero A., Puls J., Najarro F., 2002, A&A, 396, 949

Hillier D. J., Miller D. L., 1998, ApJ, 496, 407

Hillier D. J., Lanz T., Heap S. R. et al., 2003, ApJ, 588. 1039

Howarth I. D., Prinja R. K., 1989, ApJS, 69, 527

Howarth I. D., Siebert K. W., Hussain G. A. J., Prinja R. K., 1997, MNRAS, 284, 265

Hubeny I., Heap S. R., Lanz T., 1998, in ASP Conf. Ser 131, Boulder-Munich II: Properties of Hot, Luminous Stars, ed. I. D. Howarth (San Francisco, ASP), 108

Humphreys R. M., McElroy, D. B., 1984, ApJ, 284, 565

Kudritzki R.-P., Puls J., Lennon D. J. et al., 1999, A&A, 350, 970

Kudritzki R.-P., Puls J., 2000, ARA&A, 38, 613

Kudritzki, R.-P., 2002, ApJ, 577, 389

Lamers H. J. G. L. M., Snow T. P., Lindholm D. M., 1995, ApJ, 455, 269

Leitherer C., Robert, C., Drissen, L., 1992, ApJ, 401, 596

Lennon D. J., 1997, A&A, 317, 871

Lennon D. J., 1999, RMxAC, 8, 21

Markova N., Puls J., Repolust T., Markov H., 2004, A&A, 413, 693

Martins F., Schaerer D., Hillier D. J., 2002, A&A, 382, 999

Massa D., Fullerton A. W., Sonneborn G., Hutchings J.B., 2003, ApJ, 586, 996

Massey P., 2002, ApJS, 141, 81

McErlean N.D., Lennon D.J., Dufton P. L., 1999, A&A 349, 553

Prinja R. K., 1987, MNRAS, 228, 173

Prinja R. K., Barlow M. J., Howarth I. D., 1990, ApJ, 361, 607

Prinja R. K., Crowther P.A., 1998, MNRAS, 300, 828

Prinja R. K., Massa D., Fullerton A. W., 2002, A&A, 388, 587

Puls, J., Springmann, U., Lennon, M., 2000, A&AS, 141, 23

Repolust T., Puls J., Herrero A., 2004, A&A, 415, 349

Sanduleak N., 1968, AJ, 73, 246

Santolaya-Rey A. E., Puls J., Herrero A., 1997, A&A, 323, 488

Schmidt-Kaler T., 1982, in Schaifers K., Voigt H. H., eds., Landolt-Börnstein, Group VI, Vol 2b, Springer-Verlag, p. 1

Shull J. M., Van Steenberg M. E., 1985, ApJ, 294, 599

Siebert K. W., 1999, Ph.D. thesis, Univ. of London

Trundle C., Lennon D. J., Puls J., Dufton P. L., 2004, A&A, in press (TL04)

Urbaneja M. A., Herrero A., Kudritzki R.-P. et al., 2002, A&A, 386, 1019

Urbaneja M. A., Herrero A., Bresolin F. et al., 2003, ApJ, 584, L73

Vink, J. S., de Koter, A., Lamers, H. J. G. L. M., 2001, A&A, 369, 574

Walborn N. R., Nicols-Bohlin J., Panek R. J., 1985, International Ultraviolet Explorer Atlas of O-type Spectra from 1200 to 1900Å, (NASA RP1363; Washington; NASA)

Walborn N. R., Lennon D. J., Haser S. M. et al., 1995, PASP, 107, 104

Walborn N. R., Lennon D. J., Heap S. R. et al., 2000, PASP, 112, 1243

Table 1. Observational parameters of SMC targets

Star	Alias	Sp. Type	V	$B-V$	Ref.	v_r [km s^{-1}]	Instrument	Program	log N(H I) [cm^{-2}]	v_∞ [km s^{-1}]	$v_{\rm turb}$ [km s^{-1}]	$v_{\rm turb}/v_\infty$
AzV 80	–	O4-6n(f)p	13.33	−0.14	1	131	STIS	GO7437	21.7	1550	250	0.16
AzV 75	Sk 38	O5 III(f+)	12.79	−0.16	1	141	STIS	GO7437	21.7	2000	175	0.09
AzV 15	Sk 10	O6.5 II(f)	13.20	−0.22	1	115	STIS	GO7437	21.5	2125	175	0.08
AzV 83	–	O7 Iaf+	13.58	−0.13	4	118	STIS	GO7437	21.1	925	225	0.24
AzV 95	–	O7 III((f))	13.91	−0.30	1	137	STIS	GO7437	21.5	1700	250	0.15
AzV 69	Sk 34	OC7.5 III((f))	13.35	−0.22	1	130	STIS	GO7437	21.6	1750	150	0.09
AzV 327	–	O9.5 II-Ibw	13.25	−0.22	1	177	STIS	GO7437	21.0	1500	200	0.13
AzV 215	Sk 76	BN0 Ia	12.69	−0.09	3	157	STIS	GO9116	21.8	1400	275	0.20
AzV 242	Sk 85	B1 Ia	12.11	−0.13	1	176	GHRS	GO6078	–	950	175	0.18
AzV 264	Sk 94	B1 Ia	12.36	−0.15	1	131	GHRS	GO6078	–	600	250	0.42
AzV 340	–	B1 Ia	12.69	−0.07	3	211	GHRS	GO6078	–	975	150	0.15
AzV 78	Sk 40	B1 Ia+	11.05	−0.03	2	164	*IUE*-HIRES	SWP09334	–	450	200	0.44
AzV 483	Sk 156	B1.5 Ia+	11.85	−0.08	1	185	GHRS	GO6078	–	400	250	0.63
Sk 191	–	B1.5 Ia	11.86	−0.04	2	130	STIS	GO9116	21.4	425	125	0.29
AzV 210	Sk 73	B1.5 Ia	12.60	−0.02	3	173	STIS	GO9116	21.6	750	150	0.20
AzV 18	Sk 13	B2 Ia	12.46	0.03	2	138	STIS	GO9116	21.8	325	125	0.38

References. — (1) Azzopardi & Vigneau 1975, 1982; (2) Garmany et al. 1987; (3) Massey 2002; (4) Walborn et al. 2000

Note. — Stellar identifications are those of Sanduleak (1968, Sk) and Azzopardi & Vigneau (1975, 1982, AzV). Classifications for the O-type spectra are from Walborn et al. (2000); B-type classifications are from Lennon (1997), excepting AzV 483 (Lennon, 1999) and AzV 78 (from re-inspection of the blue optical data the spectrum is now classified as B1 Ia+). Radial velocities are found from the blue optical data from Lennon (1997) and an unpublished echelle spectrum of AzV 483 (using CASPEC at the ESO 3.6-m telescope). For AzV 18, 78, 483 and Sk 191 (i.e., $v_\infty < 500$) the uncertainty in v_∞ is $\pm$50 km s^{-1}and for the remainder of the sample this increases to $\pm$100 km s^{-1}.

Table 2. Terminal velocities determined for selected Galactic B-type supergiants

			This work			Haser	
Star	Spectral Type	*IUE* image	v_∞	$v_{\rm turb}$	$v_{\rm turb}/v_\infty$	v_∞	$v_{\rm turb}/v_\infty$
HD 91969	B0 Ia	SWP09076	1500	150	0.10	1550	0.09
HD 115842	B0.5 Ia	SWP27405	1125	225	0.20	1200	0.13
HD 148688	B1 Ia	SWP01871	625	175	0.28	700	0.13
HD 152236	B1.5 Ia+	SWP06500	450	175	0.39	500	0.10
HD 14818	B2 Ia	SWP09416	600	100	0.17	650	0.10

Note. — All tabulated velocities are given in km s^{-1}, typical uncertainties of v_∞ are $\pm$100 km s^{-1}.

Table 3. Escape velocities for O and early B-type SMC stars

Star	$T_{\rm eff}$ [kK]	Ref.	v_∞ [km s^{-1}]	v_{esc} [km s^{-1}]	v_∞/v_{esc}
AzV 69	33.9	3	1800	785:	2.29:
AzV 469	33.0	2	1550	657	2.36
AzV 83	32.8	3	940	534:	1.76:
AzV 232	32.0	1	1330	495	2.69
AzV 456	29.5	2	1450	482	3.01
AzV 70	28.5	2	1450	585	2.48
AzV 372	28.0	2	1550	589	2.63
AzV 215	27.0	4	1400	447	3.13
AzV 488	27.5	2	1250	455	2.75
AzV 242	25.0	5	950	359	2.65
AzV 235	24.5	2	1400	450	3.11
AzV 264	22.5	5	600	313	1.92
Sk 191	22.5	4	425	374	1.14
AzV 78	21.5	5	450	423	1.06
AzV 210	20.5	4	750	290	2.59
AzV 18	19.0	4	325	284	1.14

Note. — Stellar temperatures have been determined using non-LTE, line-blanketed model atmospheres. The values for AzV 83 and 69 are flagged as uncertain as a result of the larger SMC distance adopted in their analysis compared with the other studies.

References. — (1) Crowther et al. 2002; (2) Evans et al. 2004; (3) Hillier et al. 2003; (4) Trundle et al. 2004, (5) Trundle et al. 2004, in preparation.

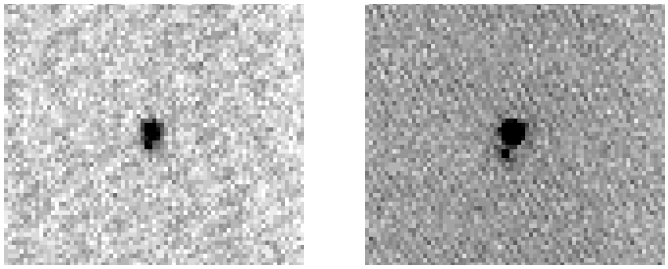

Fig. 1.— STIS acquisition images for AzV 47 (left) and AzV 216 (right). The regions shown correspond to approximately $3\farcs8 \times 2\farcs9$.

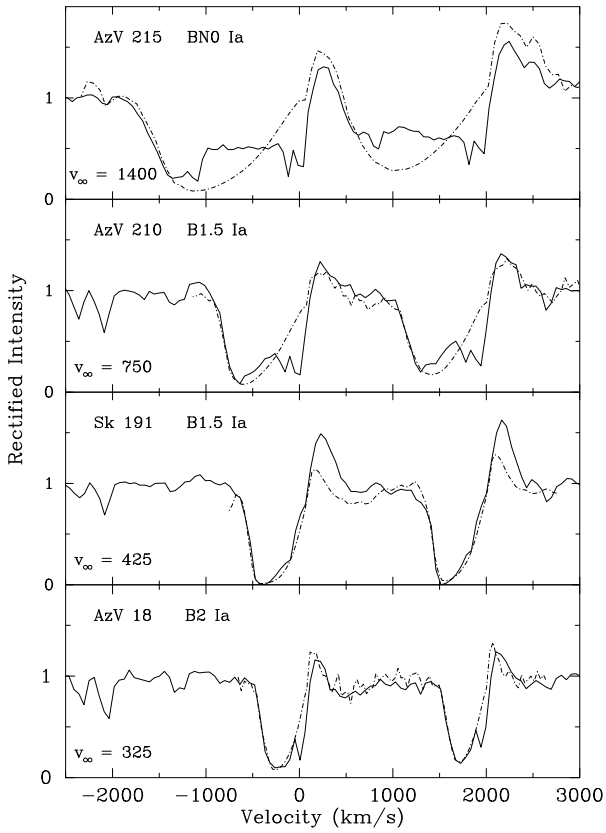

Fig. 2.— Model fits to the Si IV doublet for STIS B-type spectra. We are unable to match the morphology of AzV 215, though the same v_∞ successfully matches the C IV profile (see Figure 3).

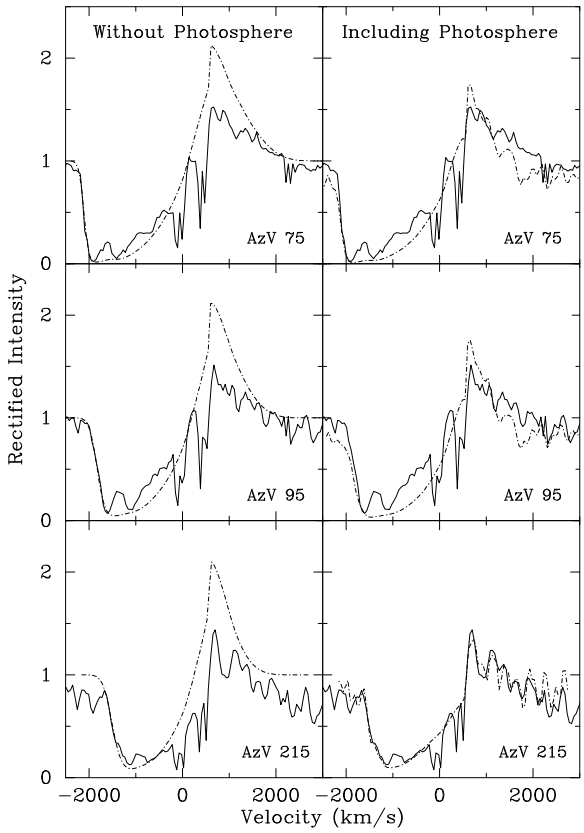

Fig. 3.— Model fits to the C IV doublet for AzV 75 [O5 III(f+)], AzV 95 [O7 III((f))] and AzV 215 [BN0 Ia]. Models were calculated without consideration of the photospheric contribution (left panel) and with inclusion of a photospheric template (right panel). The derived terminal velocities are identical.

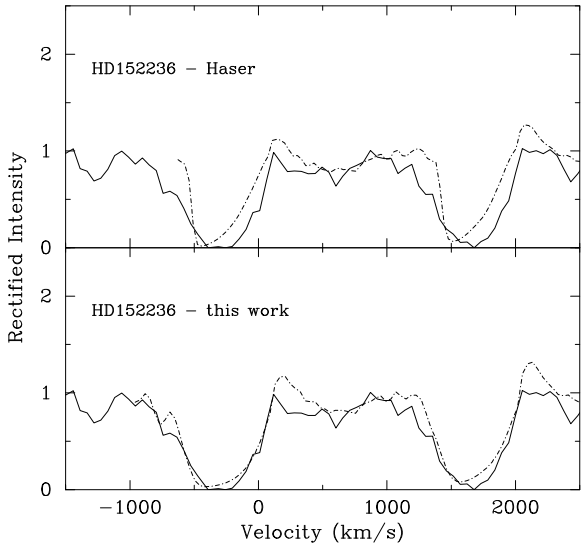

Fig. 4.— Si IV doublet of HD152236 (*solid lines*) compared with model profiles from the SEI code (*dot-dashed line*). The top panel shows a model calculated for $v_\infty = 500$ km s^{-1}, $v_{\rm turb} = 50$ km s^{-1}and $\beta = 1.5$ (Haser, 1995). The lower panel shows the model from the current study: $v_\infty = 450$ km s^{-1}, $v_{\rm turb} = 175$ km s^{-1}and $\beta = 1.0$. All profiles are shown in velocity space, relative to the blue component of the doublet, i.e., 1393.7 Å.

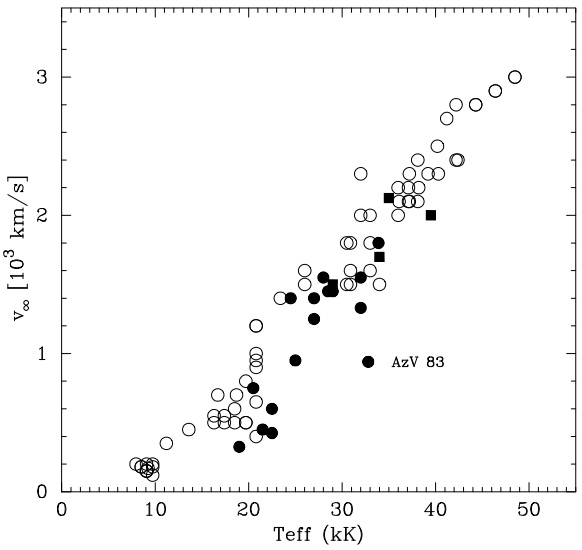

Fig. 5.— Stellar terminal velocities, v_∞, as a function of effective temperature for the current SMC sample (*solid symbols*) and for the Galactic targets of Lamers et al. (1995, *open symbols*). Squares are those stars for which the temperatures have been interpolated from published results.

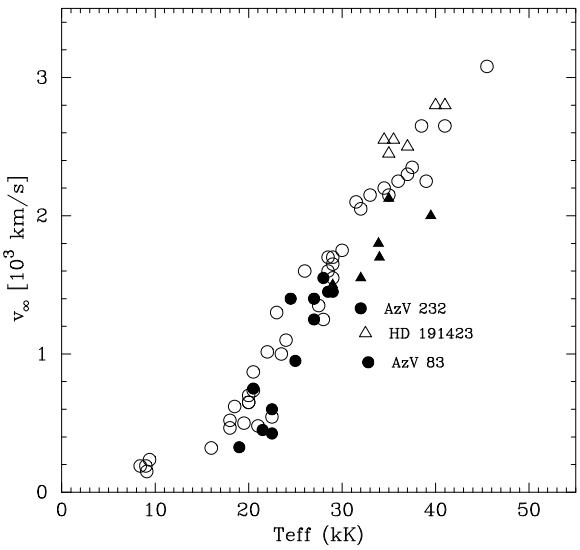

Fig. 6.— Terminal velococity v_∞ as a function of $T_{\rm eff}$ for the current SMC sample (*solid symbols*) and for published analyses of Galactic targets (*open symbols*, see text for sources). Supergiants are marked as circles, giants as triangles.

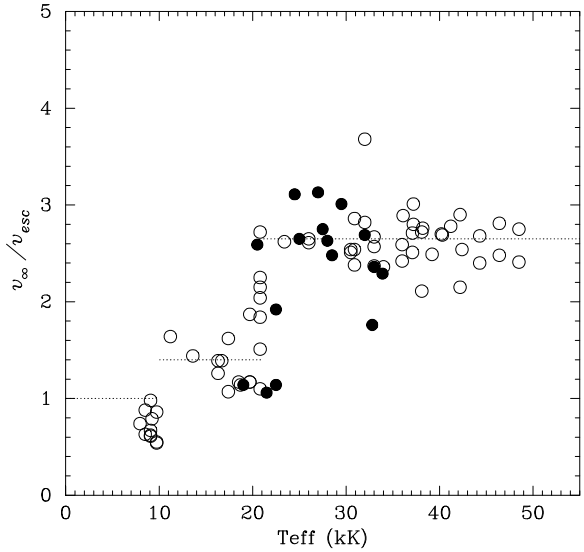

Fig. 7.— Ratio v_∞/v_{esc} as a function of $T_{\rm eff}$ from the current SMC study (*solid circles*) compared with those from the Galactic sample of Lamers et al. (1995, *open circles*). The scalings of Kudritzki & Puls (2000) are also shown (*dotted lines*).

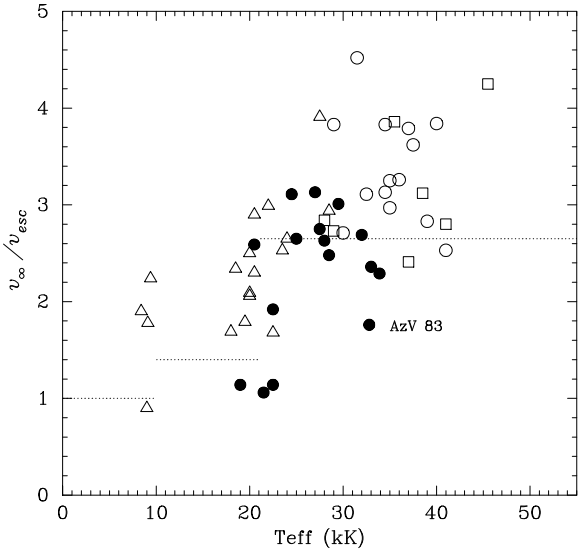

Fig. 8.— Ratio v_∞/v_{esc} as a function of $T_{\rm eff}$ from the current SMC study (*solid circles*) compared with those from the Galactic samples of Kudritzki et al. (1999, *open triangles*), Herrero et al. (2002, *open squares*) and Repolust et al. (2004, open circles). The scalings of Kudritzki & Puls (2000) are again shown (*dotted lines*).